Bollettino di Geofisica Teorica ed Applicata Vol. 56, n. 2, pp. 151-166; June 2015
DOI 10.4430/bgta0143

InSAR measurement of crustal deformation transients during the earthquake preparation processes: a review

C. Tolomei, S. Salvi, J.P. Merryman Boncori and G. Pezzo

Istituto Nazionale di Geofisica e Vulcanologia, Roma, Italy

(Received: April 15, 2014; accepted: November 4, 2014)

ABSTRACT Crustal deformation is one of the most important parameters used for the observation and modelling of the seismic cycle of strain accumulation and release. The improvements of satellite Earth observation data and methods over the last two decades, have provided a way to measure crustal movements with good accuracy and spatial coverage. In particular, multi-temporal Synthetic Aperture Radar (SAR) satellite data sets and SAR interferometric techniques have demonstrated the capacity to obtain information on the dynamics of the deformation occurring during the various phases of the seismic cycle. In the last few years a number of papers have reported the occurrence of crustal deformation transients in the inter-seismic and post-seismic periods, and have speculated on their significance in the earthquake preparation processes. The foreseen steady flow of high quality SAR data provided by new satellites as Sentinel-1 and ALOS-2 is going to provide new pieces of evidence of these elusive phenomena, stimulating further observational and analytical research. In this paper we review data, methods and applications, to give the reader a view of the advantages and the limits of InSAR measurements for the investigation of transient surface deformation patterns.

Key words: InSAR, crustal deformation, earthquake preparation, seismic cycle.

1. Introduction

During the last 25 years the technique of Interferometric Synthetic Aperture Radar (InSAR) image processing has become a widely used method for the detection of small ground movements (Bürgmann *et al.*, 2000). Especially during the last 10 years, the increased availability of new SAR instruments and satellite constellations, has stimulated a steady improvement of processing algorithms, providing measurement accuracies able to identify the small ground deformation signals associated to the different phases of the seismic cycle (Salvi *et al.*, 2012a).

In this paper we review the possibility of detecting deformation transients during the earthquake preparation processes by means of present space-based InSAR monitoring systems, and how complete and accurate this information could be in a physical or statistical modelling perspective.

We treat solely satellite SAR data, since they provide a way to cover large areas with reasonable revisit times, at lower costs than airborne data, and are thus best suited for the monitoring of earthquake preparation processes. However, most of the technical aspects are common between the two types of data.

Although the focus is on the pre-seismic phase of the seismic cycle, we also discuss the contributions of InSAR measurements to the study of the inter-seismic and post-seismic phases. In fact, by definition pre-seismic deformation transients are detected as "anomalies" with respect to accurate long-term, background time series.

The practical use of possible crustal deformation anomalies in earthquake forecasting is not presently feasible, and thus it will not be discussed in this article. We will then concentrate on deformation transients rather than earthquake precursors, since the latter term implies a generalized cause-effect relationship which still needs to be verified and explained theoretically, before it could be safely exploited for any practical use.

2. InSAR techniques for the measurement of crustal deformation

One of the most important geophysical observable measured or estimated from Earth observation (EO) data is crustal deformation. The InSAR technique can measure the projection of the deformation vector onto the Line of Sight (LoS) direction, defined as the shortest path from a given point on ground to the SAR antenna phase centre. InSAR provides some unique capabilities for the study of crustal deformation and active processes. Firstly, it can provide surface deformation maps with high spatial resolutions (5–80 m) over large areas. Secondly, InSAR is particularly sensitive to vertical displacements and finally, it is a remote-sensing technique and as such it does not require field work and can be available practically worldwide.

SAR is a coherent active microwave image instrument, which can acquire data during daytime or nighttime, and virtually under all meteorological conditions. Each SAR image pixel consists of a complex value, obtained as the vector sum (i.e., accounting for amplitude and phase) of the backscattered incident radar pulse from the elementary targets within a resolution cell. While the amplitude of the backscattered signal can be related to the surface scattering properties, its phase contains travel-time information. More precisely, although the phase in a single SAR acquisition can be considered a random variable, the phase difference between two acquisitions can be related to the changes in the geometric distance of the radar from the illuminated object, provided the backscattered signals are sufficiently correlated. InSAR has exploited this basic principle since the late 1980s (Goldstein *et al.*, 1988; Gabriel *et al.*, 1989) to measure topography and surface displacement (Bürgmann *et al.*, 2000), benefiting from the data provided by ~20 civilian or dual-use space-borne SAR sensors launched worldwide since the early 1990s.

The basic InSAR observable is called an interferogram, and represents the per-pixel phase difference between two SAR acquisitions. In general, an interferogram will contain both topographic and surface motion information; surface motion can be obtained removing topographic component either using an external DEM (e.g., Massonnet *et al.*, 1993) or using a second SAR image pair (e.g., Zebker *et al.*, 1994). In the so-called differential interferogram obtained in this way, each fringe corresponds to a LoS displacement equal to $l/2$, where l is the SAR wavelength (Fig. 1).

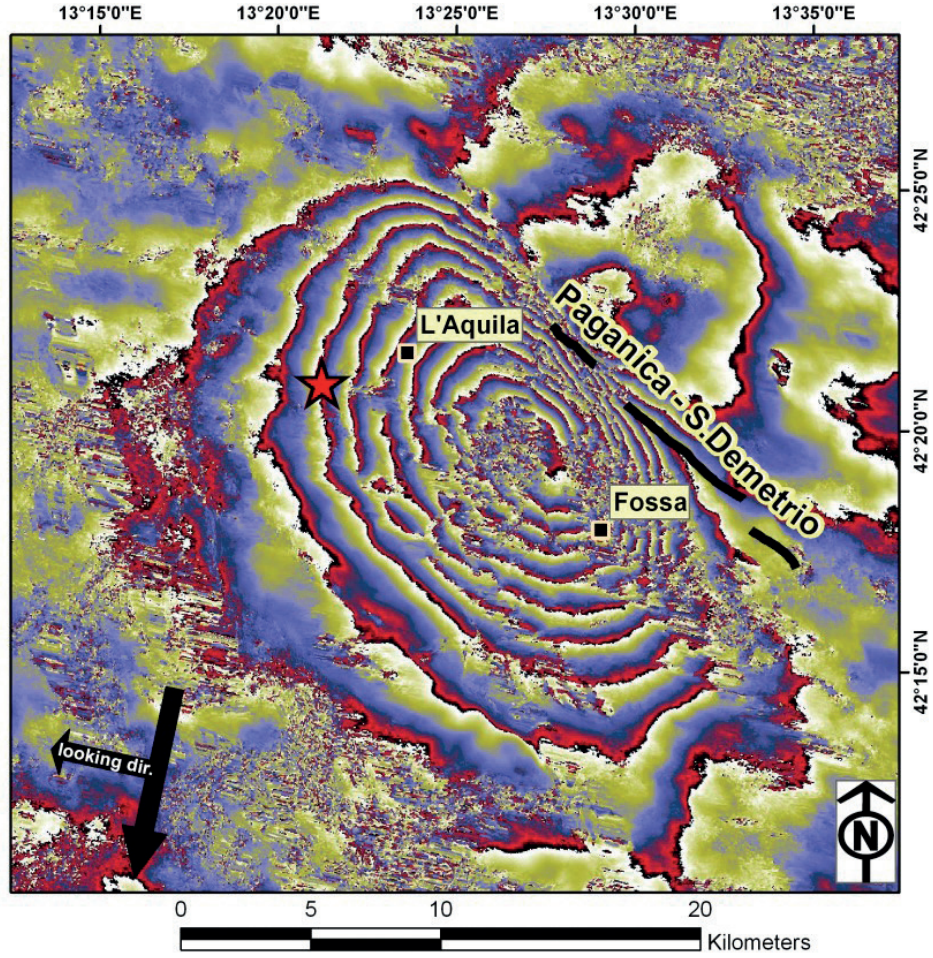

Fig. 1 - Differential interferogram showing the co-seismic fringe pattern of the M_W 6.3 L'Aquila earthquake (central Italy), occurred on April 6, 2009. Each color cycle (red to blue) corresponds to a deformation gradient of 1.6 cm, i.e., half the wavelength of the X-band COSMO-SkyMed sensor data, which was processed (from Atzori *et al.*, 2009).

Several issues however, may complicate the application of InSAR to a single image pair. Firstly, several sources (e.g., vegetation growth, ground movement, soil erosion, plowing, differences in imaging geometry) may cause the SAR phases at the two acquisitions to be statistically decorrelated (Zebker and Villasenor, 1992), and thus unrelated to the changes in the geometric distance from the radar. Secondly, phase differences are only observed modulus 2π. The recovery of the integer multiples of 2π, and thus the determination of the phase gradient between any two interferogram pixels, represents a 2D phase unwrapping problem, for which only approximate solutions can be found by automated algorithms (Chen and Zebker, 2000). Finally, the measured differences in travel times (or distances) can also be influenced by unmodeled effects, e.g., due to variable propagation velocity through the variably refractive atmosphere (mainly due to water vapor content in the troposphere and Total Electron Content in the ionosphere) and to uncertainties in the satellite position.

Several multi-temporal InSAR techniques have been proposed in the last decade, which exploit the redundancy offered by tens or hundreds of image pairs to reduce the aforementioned

limitations. The output of these techniques is a ground displacement time series, temporally referred to the first acquisition date of the image stack, and spatially referred to a reference point or area within the radar coverage.

The existing algorithms fall into two broad categories, namely the Persistent Scatterer [PS: Ferretti *et al.* (2001)] and the Small Baseline [SB: Berardino *et al.* (2002)] approaches, although more recently algorithms exploiting the basic principles of both methodologies have also been proposed (Hooper and Zebker, 2007). The aim of the PS methods is to identify coherent radar targets exhibiting a high phase stability over the whole temporal span of the observations (Ferretti *et al.*, 2001). These targets are only slightly affected by temporal and geometrical decorrelation, and often correspond to man-made structures or bare rock. In contrast, in the original SB approach (Berardino *et al.*, 2002), interferometric pairs are chosen to minimize temporal and geometric decorrelation, allowing deformation time series to be retrieved for distributed scatterers, i.e., neighboring radar resolution cells, which are not dominated by a single scatterer, and share the same backscattering properties.

Compared to single stable scatterers, a greater degree of averaging (in the order of 100 m × 100 m), yet sufficiently high for crustal deformation studies, is typically required for distributed scatterers to retain a good level of coherence, and thus to achieve high measurement accuracies (Lanari *et al.*, 2004). The latter depend on various factors, such as the type of terrain and the properties of the SAR image data stack. In the best case, both PS and SB multi temporal InSAR approaches can reach accuracies as high as 1 mm/yr (Casu *et al.*, 2006; Lanari *et al.*, 2007; Hooper *et al.*, 2012).

3. Crustal deformation during the earthquake cycle

Since the second half of the 20th century, thanks to the fast progressing technological improvement of geodetic networks and methods, the number and accuracy of crustal deformation observations in different tectonic contexts have begun to increase steadily. The new data stimulated the development of geophysical models trying to describe the characteristics of the cyclic behavior of crustal stress accumulation and release, initially proposed by Reid in his Elastic Rebound Theory (Reid, 1910).

While the physical processes and mechanisms driving the seismic cycle are still not completely understood, its existence is not questioned any more (Wang, 2007). A representation of the main processes acting during the seismic cycle in the crustal volume surrounding an active fault, is shown in Fig. 2, and provides the basis for describing four temporally distinct phases in the cycle (Thatcher, 1983):

1. the loading phase, where crustal stress slowly and gradually accumulates on the locked fault surface, is the inter-seismic phase, typically lasting hundreds to tens of thousands years. Geodetic observations of crustal strain during this phase can make important contributions to the assessment of seismic hazard, as the rate of strain accumulation on a fault may be directly related to the rate of earthquake occurrence;
2. a small number of observations has shown the presence of peculiar crustal deformation signals just before the occurrence of large earthquakes (Mogi, 1985b; Roeloffs, 2006), and this has allowed some scientists to postulate the existence of a pre-seismic phase, in which different models, generally validated by well confined laboratory experiments,

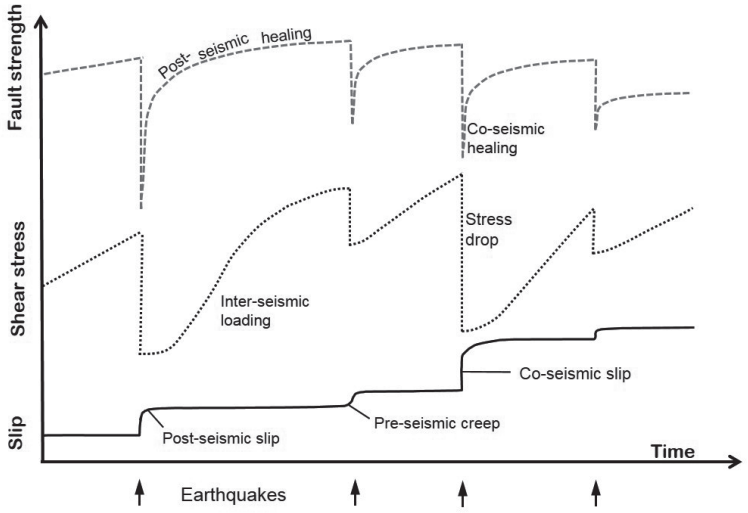

Fig. 2 - Idealized representation of the seismic cycle. During the seismic cycle the fault strength and shear stress increase with time. The fault failure is the result of the complex interaction between the loading stress and the evolution of the fault strength with time. Both are controlled by several non-linear processes acting at a very different scales (modified from Di Toro *et al.*, 2012).

predict the occurrence of a variety of phenomena, potentially affecting the solid Earth and the atmosphere (Nur, 1972; Scholz *et al.*, 1973; Miachkin *et al.*, 1975; Crampin *et al.*, 1980, 1984; Das and Scholz, 1981; Roeloffs, 2006);

3. once sufficient shear stress on the fault has accumulated to exceed the fault's frictional strength, the rupture is initiated and propagates over the finite fault plane, causing a rapid drop of the stress level. The inter-seismic phase then gives way to the co-seismic phase, which is accompanied by rapid volume (and in general also surface) strain. Studies of this phase of the seismic cycle are very important to improve the knowledge of the earthquake source processes;
4. finally, after the earthquake, the cycle enters the post-seismic phase. In this interval, lasting up to several decades, the stress changes imparted by the earthquake are relaxed, generating crustal and lithospheric deformation that is significantly faster than the inter-seismic rates. Study of this period of the seismic cycle can lead to the understanding of the constitutive laws and parameters of the crust and uppermost mantle, fundamental to our knowledge of how the lithosphere responds to stress.

Crustal deformation occurs at different temporal and spatial scales, depending on the various phases. During the inter-seismic phase the long-term tectonic stress accumulation occurs at the scale of entire regions (hundreds of kilometres), generating slow-varying crustal deformation patterns. This type of deformation is typically considered steady-state, but its accurate measurement is an essential prerequisite for any short-term transient detection.

During the pre-seismic phase, transient deformation signals may occur at mid-term (months to years) or short-term (seconds to weeks) scales. The presence of mid- or short-term transient crustal deformation signals, which are considered anomalous with respect to the long-term deformation time series, has been fragmentarily reported in the literature, with different levels of quality and reliability. Most of the reports deal with anomalies in the supposedly steady inter-seismic deformation rates, often occurring in the temporal and spatial vicinity of large earthquakes. Mid-term deformation transients have been measured over months or years, and on spatial scales of tens or hundreds of kilometres (Gu *et al.*, 2009; Ozawa *et al.*, 2012; Hashimoto, 2013). Their relevance to the earthquake preparation processes is in some cases supported by

modelling, as for the aseismic or slow slip events occurring on the down-dip part of large faults before the mainshocks (Roeloffs, 2006; Miyazaki *et al.*, 2011; Ozawa *et al.*, 2012).

In the post-seismic phase, thanks to the increased quality and density of Continuous Global Positioning Sistem (CGPS) and InSAR data and of their analysis methods, new observations of long-term and short-term deformation transients have been obtained worldwide (Peltzer *et al.*, 2001; Ozawa *et al.*, 2002; Miyazaki *et al.*, 2003; Bernard *et al.*, 2004; Dragert *et al.*, 2004; Larson *et al.*, 2004; Cakir *et al.*, 2005; Pritchard and Simons, 2006; Calais *et al.*, 2008; Furuya and Satyabala, 2008; Ozawa *et al.*, 2012; Salvi *et al.*, 2012a). Post-seismic deformation transients are typically generated by different processes, as fault after-slip, poroelastic rebound, or, at a larger scale, viscoelastic relaxation of the lower crust and the upper mantle (Pollitz *et al.*, 2000; Barbot and Fialko, 2010). The co- and post-seismic stress redistribution has gained considerable attention in the last 20 years, following the appreciation of the importance of stress triggering mechanism of large aftershocks (Steacy *et al.*, 2005). At present one of the most intriguing research fields regards the contribution of post-seismic stress redistribution to estimate the spatially varying aftershock probabilities following large earthquakes.

4. InSAR measurement of transient deformation during the earthquake cycle

4.1. The pre-earthquake period

In this chapter we will discuss about the deformation accumulating on a given fault or region before a large earthquake occurs, comprising either the steady, long-term inter-seismic strain accumulation, and the shorter-term transients (lasting from years to seconds), which may or may not culminate into earthquakes.

The capacity of InSAR methods to measure the inter-seismic strain accumulation has been proved in several cases [see: Salvi *et al.* (2012a) for a review of results obtained using ERS/ENVISAT data], although further improvements are required especially for the removal of atmospheric disturbances. Accuracies of 1-2 mm/yr could be achieved in favourable conditions, and Sentinel-1's larger swaths and improved temporal coverage are expected to increase these levels further (Salvi *et al.*, 2012b).

The use of InSAR for inter-seismic deformation measurement has concentrated mainly on segments of large strike-slip faults [e.g., the Chaman fault in Pakistan (Szeliga *et al.*, 2012), the Haiyuan fault system in north-eastern Tibet (Jolivet *et al.*, 2013), the North Anatolian fault (Wright *et al.*, 2001; Walters *et al.*, 2011; Kaneko *et al.*, 2013), the Denali fault in Alaska (Biggs *et al.,* 2007)]. Other studies, not concerning purely strike-slip faults, include the western part of the Doruneh fault system, north-eastern Iran (Pezzo *et al.*, 2012), the Longitudinal Valley, Taiwan, (Peyret *et al.*, 2011; Champenois *et al.*, 2012), the Abruzzi region in central Italy (Hunstad *et al.*, 2009).

From the technique point of view, most of the inter-seismic deformation studies apply Small Baseline methods (Hunstad *et al.*, 2009; Gourmelen *et al.*, 2010; De Michele *et al.*, 2011; Manzo *et al.*, 2012; Jolivet *et al.*, 2013), but PS methods have also been applied successfully (Motagh *et al.*, 2007; Peyret *et al.*, 2011; Champenois *et al.*, 2012). Depending on the area of interest, the main challenges faced by the above mentioned studies, to a greater or lesser degree, have been:

- distinguishing long spatial wavelength (>10 km) inter-seismic deformation from errors due to satellite platform orbital uncertainties and slowly-varying atmospheric phase delays;
- mitigating tropospheric delays correlated with topography, due to temporal variations of tropospheric stratification;
- mitigating phase unwrapping errors;
- mitigating turbulent tropospheric delays and characterizing the spatial correlation introduced by this error source in the measurements.

Concerning the measurement of long-wavelength deformation signals, essentially three approaches are successfully used: calibration with GPS measurements, provided that a sufficiently dense network is available (e.g., Fialko, 2004; Manzo *et al*., 2012); estimation from SAR measurements at a sufficient distance from the expected area of highest deformation (e.g., Walters *et al*., 2011; Pezzo *et al*., 2012); use of slip models (Biggs *et al*., 2007; Cavalié *et al*., 2008; Wang *et al*., 2009; Jolivet *et al*., 2013).

In most cases, when tropospheric delays correlated with topography are accounted for, they are modelled as a phase term linearly correlated with elevation. The scaling coefficient is estimated directly from SAR interferograms, using a network approach, i.e., exploiting the redundancy of the interferometric pairs to derive a joint estimation for the scaling factor of each interferogram (Elliott *et al*., 2008; Wang and Wright, 2012; Jolivet *et al*., 2013). Global numerical weather model data is used by some authors (e.g., Jolivet *et al*., 2013) as a validation for the estimated scaling coefficients.

Phase unwrapping errors are mostly mitigated by data redundancy, although network approaches for error mitigation have been applied (Doin *et al*., 2011; Wang and Wright, 2012).

Finally, turbulent tropospheric delays could be mitigated in stacking techniques by data redundancy and low-pass temporal filtering. The latter approach however could smear any transient signal in the displacement time series, and must be applied with care. Characterization of this error source, in terms of the spatial covariance function of the delay, is equally important, since it can be used for InSAR data selection, as well as in subsequent modelling (Jolivet *et al*., 2013).

Due to the difficulty in accounting for the above issues, the InSAR time-series analysis for inter-seismic deformation measurement works better for fault systems with high slip rates (greater than several mm/yr), for which the measurable deformation signal is well over the noise.

The presence of shorter term transients with intensities from mm/yr to cm/yr has been observed or suggested initially by classical geodetic methods (Mogi, 1985a; Linde and Sacks, 2002), then measured by CGPS (Yu *et al*., 2001; Miyazaki *et al*., 2003), and recently captured also by InSAR (Pritchard and Simons, 2006; Jolivet *et al*., 2013). Nowadays, modelling and theoretical developments (Liu and Rice, 2007; Peng and Gomberg, 2010) suggest that many of these deformation events can be generated by aseismic slip or slow-slip events, often located in the deeper parts of a larger fault which later releases seismic slip (Roeloffs, 2006; Miyazaki *et al*., 2011). While the possible cause-effect relationship between these transients and the mainshock is not yet clear, there is considerable interest in their measurement and analysis for the comprehension of the dynamics of the rupture process.

In this field, InSAR measurements could be very effective thanks to their good spatial coverage; however, the repeat pass of the present satellites presently limits the resolving capacity to transients lasting several days at minimum (using the COSMO-SkyMed constellation).

One other important issue concerns the lack of a routine acquisition plan for some satellite

missions. Since the start of the InSAR era, only the ERS, ENVISAT, and ALOS missions have implemented a nearly global background acquisition plan, under which many seismic regions of the Earth were constantly monitored, although not always with full success. Other missions, such as Radarsat, TerraSAR-X, COSMO-SkyMed, which mostly acquire on demand, can dedicate, for technical and practical reasons, only limited resources to background acquisitions, and cannot provide a global continuous long-term coverage. For instance COSMO-SkyMed, which at present is the system allowing the highest temporal resolution (in the best case as high as one day) over the same target, has a theoretical average daily acquisition capability of 375 Stripmap images, for each satellite. In Stripmap mode (the main mode used for InSAR) each COSMO-SkyMed satellite can acquire on each orbit at most 1/10 of the land pass (~ 4000 km). The actual amount of images acquired may be further reduced by limited bandwidth resources for the data down-link to the ground stations under visibility, as well as by acquisition or down-link conflicts with other acquisition requests (military or commercial).

These issues will be mostly solved by the new ESA Sentinel-1 satellite, which will provide a constant 12-day (6-day with the second satellite) repeat pass over all of Europe and a 24-day (12-day) one for most of the emerged lands (Torres *et al.*, 2012). The Sentinel-1 long-term operational monitoring will certainly foster important observations of mid-term crustal deformation transients at the global scale.

4.2. The co- and post-seismic phases

The capacity of InSAR to accurately measure the static displacement field generated by seismic dislocations has been widely demonstrated for over 60 earthquakes since 1994 (Weston *et al.*, 2011). Until the development of the multitemporal InSAR techniques this was done exclusively using classical interferometric analysis based on a pair of pre- and post-event images, which, however, typically spanned a period containing part of the early post-seismic displacements. Then, the possibility to generate a time series of the deformation including the earthquake, allowed a more precise separation of the actual co-seismic displacement from the post-seismic one (Atzori *et al.*, 2009).

In the last 15 years, InSAR time-series have been used to investigate the post-seismic deformation of several large strike-slip events, such as the M_W 7.2 Landers in 1992 (Massonnet *et al.*, 1994; Fialko, 2004), the M_W 7.5-7.6 Manyi event in 1997 (Ryder *et al.*, 2007), the M_W 7.1 Hector Mine event in 1999 (e.g., Pollitz *et al.*, 2001; Jacobs *et al.*, 2002), the M_W 7.6 Izmit event in 1999 (e.g., Bürgmann *et al.*, 2002a; Ergintav *et al.*, 2002; Hearn *et al.*, 2002), and the M_W 7.9 Denali event in 2002 (Pollitz, 2005; Biggs *et al.*, 2009). A minor number of dip-slip faults has been investigated: the M_W 7.2 El Mayor-Cucapah event in 2010 (Gonzalez-Ortega *et al.*, 2014), the M_W 7.2 Van event (Doğan *et al.*, 2014), the M_W 6.3 Damxung event (Bie *et al.*, 2014), the M_W 6.3 L'Aquila event (Reale *et al.*, 2011; D'Agostino *et al.*, 2012).

Recently, using the high sensitivity to deformation of the X-band and the short temporal baselines, COSMO-SkyMed imagery has been used to measure small post-seismic deformation following the M_W 5.9 Emilia 2012 event in northern Italy (Fig. 3). For this sequence a classical two pass InSAR analysis revealed the occurrence of a slow or aseismic slip event which could have played a role in triggering one of the main shocks of the sequence (Pezzo *et al.*, 2013). Unfortunately, this transient could not be analyzed in more detail since there was no dense COSMO-SkyMed coverage of the area, and GPS stations were too scattered to capture this local pattern.

Geodetically determined post-seismic deformation has been modelled as afterslip on a discrete plane (e.g., Bürgmann *et al*., 2002b), creep in a viscous or viscoelastic shear zone (e.g., Hearn *et al*., 2002), viscoelastic relaxation in the lower crust/upper mantle (e.g., Pollitz *et al*., 2000), and poro-elastic rebound (e.g., Jonsson *et al*., 2003). In some cases, it has been possible to distinguish multiple mechanisms, operating often with different time constants, e.g., poro-elastic rebound coupled with localized deep shear (e.g., Fialko, 2004); poro-elastic rebound, afterslip and shallow volumetric contraction (Fielding *et al*., 2009). The use of InSAR in the study of post-seismic movements in subduction areas has led to an improved understanding of the source mechanism in transitional zones (Béjar-Pizarro *et al*., 2010) characterized by alternating transient aseismic shear and seismic slip (Hyndman and Wang, 1993). Transient aseismic slip is also observed as post-seismic afterslip in both the lower region and the upper region of the seismogenic zone, apparently in areas surrounding the main asperity characterized by high coseismic slip (e.g., Chlieh *et al*., 2004; Miyazaki *et al*., 2004; Baba *et al*., 2006; Hsu *et al*., 2006; Pritchard and Simons, 2006).

5. Operational InSAR monitoring of transient deformation during the earthquake cycle

InSAR monitoring techniques have the advantage of being independent of field campaigns (although ground data may be required for validation), but at the same time they depend on satellite imagery which is provided by very expensive missions, whose development requires several years at least, and whose primary mission objective is not necessarily scientific research. In this section we discuss some practical issues concerning the actual operational use of SAR data for the monitoring of earthquake preparation processes, with some reference to the Italian situation.

Concerning past InSAR data, the main source of useful imagery is provided by the ESA ERS-1, ERS-2 and ENVISAT-ASAR sensors (C-band, 5.3 GHz), which all together span nearly 20 years, from the end of 1991 to July 2011. For the main parts of the missions the repeat cycle of both ERS and ASAR missions was 35 days.

Presently a C-band Canadian sensor (Radarsat-2), two German X-band instruments (TerraSAR-X and TanDEM-X), the Japanese L-band PALSAR-2 sensor on board ALOS-2, the European Space Agency C-band Sentinel-1A SAR, and the four COSMO-SkyMed X-band sensors managed by the Italian Space Agency (ASI) are operational. The latter are playing an important role for InSAR applications, particularly on the Italian territory. Since the end of 2010, ASI implemented a nationwide monitoring plan (Map Italy), devised in cooperation with the Italian Civil Protection (DPC) for the various natural risks. The goal of the plan was to cover all land areas of Italy with COSMO-SkyMed strip-map imagery, providing a revisit time of 16 days, in order to create an operational archive for the management of hydrological, volcanic and seismic emergencies. The continuity of the Map Italy archive is extremely important for both the standard two pass InSAR applications and for the multitemporal (time series) ones. Besides this background acquisition plan, COSMO has provided a wealth of imagery in connection with major seismic events in Italy, e.g., L'Aquila and Emilia events, and abroad, e.g., for the New Zealand 2010-2011 sequence (Salvi *et al*., 2012a) and the Great Tohoku earthquake, Japan (Salvi *et al*., 2011).

The enhanced capacities provided by continuously improved InSAR data and techniques

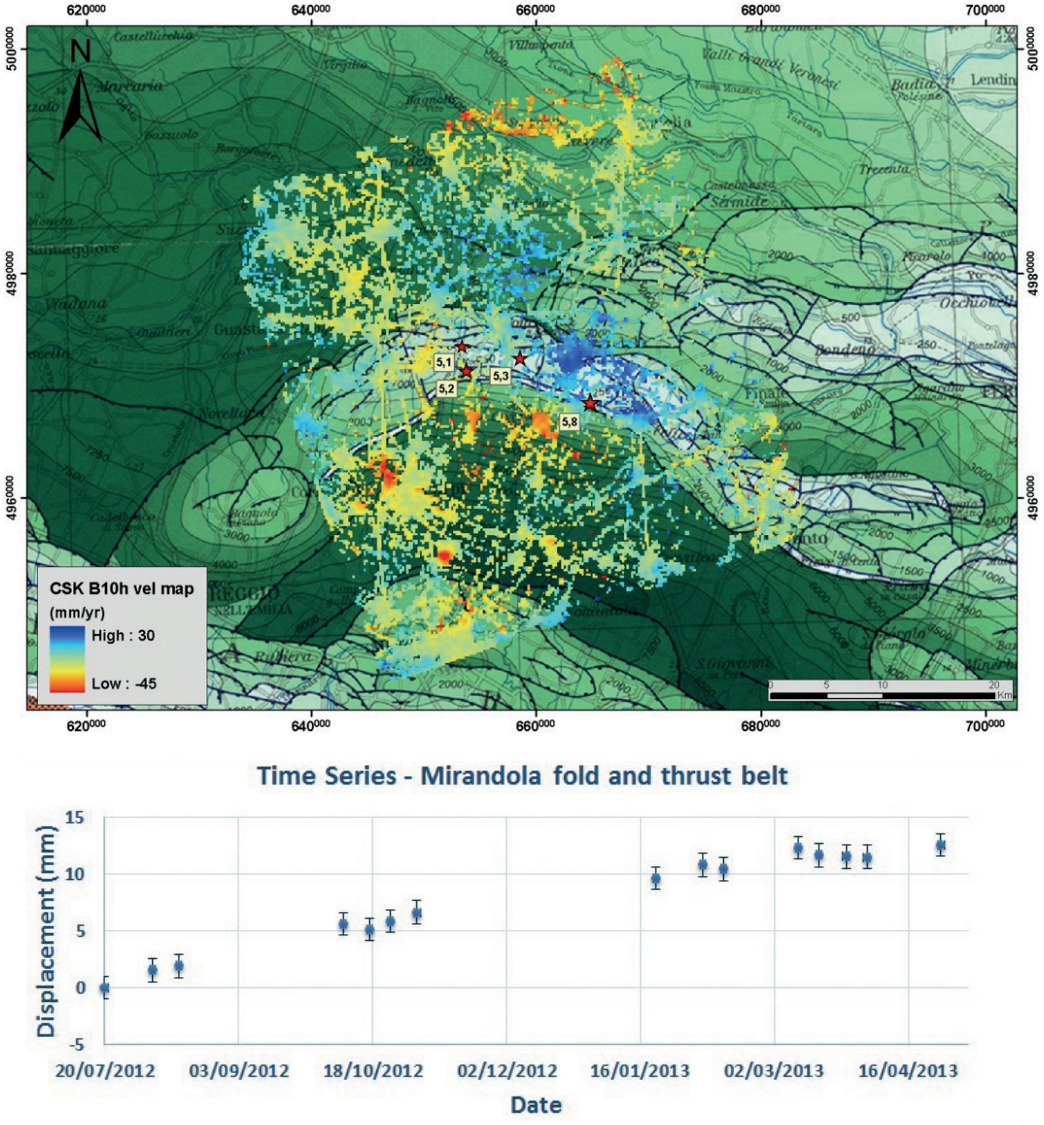

Fig. 3 - Above map: COSMO-SkyMed ascending mean velocity covering the first 11 months of the Emilia post-seismic period, superimposed to the geo-structural model (Bigi *et al.*, 1983). A clear post-seismic LoS "uplift" occurs in the same area affected by the co-seismic deformation of the Mirandola M_W 5.8 earthquake fault. Local subsidence signals are also evident in the urbanized areas of the region. Lower graph: a displacement time series in the uplifting area (blue colours) over the Mirandola thrust.

for the monitoring of crustal deformation transients are of great importance for stimulating new research on the earthquake preparation processes. However, the use of these techniques on a global scale (i.e., in a wide variety of tectonic settings) is still challenging, due to several issues discussed below. These challenges elicit strict requirements on SAR missions (current and future), particularly in terms of acquisition frequency and regularity, and further development of the current multi-temporal SAR processing techniques.

The first issue is related to the seismotectonic setting. In many areas of the world, seismic sources exhibit inter-seismic slip rates, estimated on a geological basis, varying between 1 mm/yr and few mm/yr, with surface deformation gradients ranging between 0.01-0.1 mm/yr/km.

These values are at least one order of magnitude smaller than those measured by most of the InSAR inter-seismic studies mentioned in section 4.

A second issue concerns the discrimination between long spatial wavelength inter-seismic deformation gradients and long-wavelength phase delay signals, due to atmospheric propagation and orbital artifacts. These signals can be easily separated using CGPS data from dense networks, especially where the crustal deformation signal is dominated by the presence of a regional fault (e.g., the San Andreas or North Anatolian faults). However, in many tectonic settings there is no dominating regional fault and the CGPS coverage is rather sparse, and the isolation of low gradient tectonic signals becomes challenging.

To this end, the 250-km swath of Sentinel-1 will be beneficial, since it will be easier to identify areas with no deformation and there will be a better chance to include CGPS stations in a single coverage.

Thirdly, to minimize the loss of coherence due to many vegetated and/or cultivated areas, and to the high topographic relief characteristic of the most active areas, stringent acquisition requirements would be necessary. For instance, repeat-pass cycles and spatial baselines should be as small as possible (few days, few tens of metres), and acquisition look angles should preferably be between 30° and 50° in mountainous regions. Also in this case the C-band Sentinel 1 mission shows two desirable properties: a revisit time of 12 days (6 with the second satellite, but only over Europe) and a planned orbital tube diameter of 100 m.

In summary, the Sentinel-1 data are expected to boost the global monitoring capacity for deformation transients with periods of several tens of days; for transients with shorter periods (few tens of days) and with small amplitudes (few mm), frequent X-band data as those provided by COSMO-SkyMed will continue to play an important role, especially if a more stringent control of the orbital tube is implemented.

6. Conclusions

The presently available InSAR data can effectively measure deformation transients with periods of few-to-several tens of days. The shorter period signals can presently be investigated only using continuous GPS, which however may lack the necessary spatial sampling to fully investigate the deformation causes. The CGPS data are also very useful to model non-tectonic signals during the SAR data processing, and therefore CGPS must be used in synergy with InSAR methods whenever possible.

As regards the data availability, in 2014 a new InSAR era has started, with the successful deployment of the European Sentinel-1 SAR satellite (a second Sentinel-1B mission is scheduled for 2015), able to provide SAR images for most seismic areas of the world with constant repeat pass, for many years in the future. The improved SAR data availability, the larger coverage, the constant temporal sampling provided by the Sentinel-1 sensors will generate a strong increase in the observation of crustal deformation transients worldwide, providing new high quality data for developing and testing models of the earthquake preparation processes. However, even with the successful launch of Sentinel-1B, the revisit time will remain relatively high (6 days in Europe, but in general 12 days) and will not allow to investigate these phenomena in sufficient detail. An important role in this respect could still be played by

the X-band SAR constellations, provided that their data policy is improved to allow an easier data access for scientific research. Such elusive signals could be detected only by setting up long-term monitoring experiments over several tectonic areas of the world, acquiring with the shortest possible repeat pass.

Acknowledgments. This work has been carried out in the framework of the S3 project (DPC-INGV) "Short-term earthquake forecasting", years 2012-13. The InSAR results have been obtained using COSMO-SkyMed products, © ASI (Italian Space Agency) provided under license of ASI under the SIGRIS project. G. Pezzo and J.P. Merryman Boncori have been supported by the ESA CHARMING project. Scientific papers founded by DPC do not represent its official opinion and policies.

REFERENCES

Atzori S., Hunstad I., Chini M., Salvi S., Tolomei C., Bignami C., Stramondo S., Trasatti E., Antonioli A. and Boschi E.; 2009: *Finite fault inversion of DInSAR coseismic displacement of the 2009 L'Aquila earthquake (central Italy)*. Geophys. Res. Lett., **36**, L15305, doi:10.1029/2009GL039293.

Baba T., Hirata K., Hori T. and Sakaguchi H.; 2006: *Offshore geodetic data conducive to the estimation of the afterslip distribution following the 2003 Tokachi-oki earthquake*. Earth Planet. Sci. Lett., **241**, 281-292.

Barbot S. and Fialko Y.; 2010: *A unified continuum representation of post-seismic relaxation mechanisms: semi-analytic models of afterslip, poroelastic rebound and viscoelastic flow*. Geophys. J. Int., **182**, 1124-1140.

Béjar-Pizarro M., Carrizo D., Socquet A. and Armijo R.; 2010: *Asperities and barriers on the seismogenic zone in North Chile: state of the art after the 2007 M_W 7.7 Tocopilla earthquake inferred by GPS and InSAR data*. Geophys. J. Int., **183**, 390-406.

Berardino P., Fornaro G., Lanari R. and Sansosti E.; 2002: *A new algorithm for surface deformation monitoring based on small baseline differential SAR interferograms*. IEEE Trans. Geosci. Remote Sens., **40**, 2375-2383.

Bernard P., Boudin F., Sacks S., Linde A., Blum P.A., Courteille C., Esnoult M.F, Castarede H., Felekis S. and Billiris H.; 2004: *Continuous strain and tilt monitoring on the Trizonia Island, Rift of Corinth, Greece*. CR Geosci., **336**, 313-323.

Bie L., Ryder I., Nippress S.E. and Bürgmann R.; 2014: *Coseismic and post-seismic activity associated with the 2008 MW 6.3 Damxung earthquake, Tibet, constrained by InSAR*. Geophys. J. Int., **196**, 788-803.

Biggs J., Wright T., Lu Z. and Parsons B.; 2007: *Multi-interferogram method for measuring interseismic deformation: Denali Fault, Alaska*. Geophys. J. Int., **170**, 1165-1179, doi:10.1111/j.1365-246X.2007.03415.x

Biggs J., Bürgmann R., Freymueller J.T., Lu Z., Parsons B., Ryder I., Schmalzle G. and Wright T.; 2009: *The postseismic response to the 2002 M 7.9 Denali Fault earthquake: constraints from InSAR 2003-2005*. Geophys. J. Int., **176**, 353-367, doi:10.1111/j.1365-246X.2008.03932.x.

Bigi G., Bonardi G., Catalano R., Cosentino D., Lentini F., Parotto M., Sartori R., Scandone P. and Turco E. (eds); 1983: *Structural Model of Italy 1:500,000, Sheet 1*. C.N.R., Progetto Finalizzato Geodinamica, SELCA, Firenze, Italy.

Bürgmann R., Rosen P.A. and Fielding E.J.; 2000: *Synthetic aperture radar interferometry to measure Earth's surface topography and its deformation*. Ann. Rev. Earth Planet. Sci., **28**, 169-209.

Bürgmann R., Ayhan M.E., Fielding E.J., Wright T.J., McClusky S., Aktug B., Demir C., Lenk O. and Türkezer A.; 2002a: *Deformation during the 12 November 1999, Düzce, Turkey earthquake, from GPS and InSAR data*. Bull. Seismol. Soc. Am., **92**, 161-171.

Bürgmann R., Ergintav S., Segall P., Hearn E.H., McClusky S., Reilinger R.E., Woith H. and Zschau J.; 2002b: *Time-space variable afterslip on and deep below the Izmit earthquake rupture*. Bull. Seismol. Soc. Am., **92**, 126-137.

Cakir Z., Akoglu A.M., Belabbes S., Ergintav S. and Meghraoui M.; 2005: *Creeping along the Ismetpasa section of the North Anatolian Fault (western Turkey): rate and extent from InSAR*. Earth Planet. Sci. Lett., **238**, 225-234.

Calais E., d'Oreye N., Albaric J., Deschamps A., Delvaux D., Deverchere J., Ebinger C., Ferdinand R.W., Kervyn F., Macheyeki A.S., Oyen A., Perrot J., Saria E., Smets B., Stamps D.S. and Wauthier C.; 2008: *Aseismic strain accommodation by slow slip and dyking in a youthful continental rift, East Africa*. Nature, **456**, 783-787, doi:10.1038/nature07478.

Casu F., Manzo M. and Lanari R.; 2006: *A quantitative assessment of the SBAS algorithm performance for surface deformation retrieval from DInSAR data*. Remote Sens. Environ., **102**, 195-210.

Cavalié O., Lasserre C., Doin M.P., Peltzer G., Sun J., Xu X. and Shen Z.K.; 2008: *Measurement of interseismic strain across the Haiyuan fault (Gansu China) by InSAR*. Earth and Planetary Science Letters, **275**, 246–257.

Champenois J., Fruneau B., Pathier E., Deffontaines B., Lin K.-C. and Hu J.-C.; 2012: *Monitoring of active tectonic deformations in the Longitudinal Valley (eastern Taiwan) using Persistent Scatterer InSAR method with ALOS PALSAR data*. Earth Planet. Sci. Lett., **337**, 144-155.

Chen C.W. and Zebker H.A.; 2000: *Network approaches to two-dimensional phase unwrapping: intractability and two new algorithms*. March Journal of the Optical Society of America, **A 17**, 401–414.

Chlieh M., de Chabalier J.B., Ruegg J.C., Armijo R., Dmowska R., Campos J. and Feigl K.; 2004: *Crustal deformation and fault slip during the seismic cycle in the North Chile subduction zone, from GPS and InSAR observations*. Geophys. J. Int., **158**, 695-711.

Crampin S., Evans R., Üçer B., Doyle M., Davis J.P., Yegorkina G.V. and Miller M.; 1980: *Observations of dilatancy-induced polarization anomalies and earthquake prediction*. Nature, **286**, 874-877.

Crampin S., Evans R. and Atkinson B.K.; 1984: *Earthquake prediction: a new physical basis*. Geophys. J. R. Astron. Soc., **76**, 147-156.

D'Agostino N., Cheloni D., Fornaro G., Giuliani R. and Reale D.; 2012: *Space-time distribution of afterslip following the 2009 L'Aquila earthquake*. J. Geophys. Res., Solid Earth, **117**, B02402.

Das S. and Scholz C.H.; 1981: *Theory of time dependent rupture in the Earth*. J. Geophys. Res., **86**, 6039-6051.

De Michele M., Raucoules D., Rolandone F., Briole P., Salichon J., Lemoine A. and Aochi H.; 2011: *Spatiotemporal evolution of surface creep in the Parkfield region of the San Andreas Fault (1993-2004) from synthetic aperture radar*. Earth Planet. Sci. Lett., **308**, 141-150.

Di Toro G., Mittempergher S., Ferri F., Mitchell T.M. and Pennacchioni G.; 2012: *The contribution of structural geology, experimental rock deformation and numerical modelling to an improved understanding of the seismic cycle*. J. Struct. Geol., **38**, 3-10, doi:10.1016/j.jsg.2012.01.025.

Doğan U., Demir D.Ö., Çakir Z., Ergintav S., Özener H., Akoğlu A.M., Nalbant S. and Reilinger R.; 2014: *Postseismic deformation following the M_W 7.2 October 23, 2011 Van earthquake (Turkey): evidence for aseismic fault reactivation*. Geophys. Res. Lett., **41**, 2334-2341.

Doin M.P., Lodge F., Guillaso S., Jolivet R., Lasserre C., Ducret G., Grandin R., Pathier R. and Pinel V.; 2011: *Presentation of the small baseline NSBAS processing chain on a case example: the Etna deformation monitoring from 2003 to 2010 using Envisat data*. In: Proc. 'Fringe 2011 Workshop', Frascati, Italy.

Dragert H., Wang K. and Rogers G.; 2004: *Geodetic and seismic signatures of episodic tremor and slip in the northern Cascadia subduction zone*. Earth Planets Space, **56**, 1143-1150.

Elliott J.R., Biggs J., Parsons B. and Wright T.J.; 2008: *InSAR slip rate determination on the Altyn Tagh Fault, northern Tibet, in the presence of topographically correlated atmospheric delays*. Geophys. Res. Lett., **35**, L12309, doi:10.1029/2008GL033659.

Ergintav S., Bürgmann R., McClusky S., Çakmak R., Reilinger R.E., Lenk O., Barka A. and Özener H.; 2002: *Postseismic deformation near the Izmit earthquake (17 August 1999, M 7.5) rupture zone*. Bull. Seismol. Soc. Am., **92**, 194-207.

Ferretti A., Prati C. and Rocca F.; 2001: *Permanent scatterers in SAR interferometry*. IEEE Trans. Geosci. Remote Sens., **39**, 8-20.

Fialko Y.; 2004: *Evidence of fluid-filled upper crust from observations of postseismic deformation due to the 1992 M_W 7.3 Landers earthquake*. J. Geophys. Res., **109**, B08401, doi:10.1029/2003JB002985.

Fielding E.J., Lundgren P.R., Bürgmann R. and Funning G.J.; 2009: *Shallow fault-zone dilatancy recovery after the 2003 Bam, Iran earthquake*. Nature, **458**, 64-68.

Furuya M. and Satyabala S.P.; 2008: *Slow earthquake in Afghanistan detected by InSAR*. Geophys. Res. Lett., **35**, L06309, doi:10.1029/2007GL033049.

Gabriel A.K., Goldstein R.M. and Zebker H.A.; 1989: *Mapping small elevation changes over large areas—differential radar interferometry*. J. Geophys. Res. **94**, 9183–91.

Goldstein R.M., Zebker H.A. and Werner C.L.; 1988: *Satellite radar interferometry: two-dimensional phase unwrapping*. Radio Sci., **23**, 713-720.

Gonzalez-Ortega A., Fialko Y., Sandwell F.A., Nava-Pichardo F.A., Fletcher J., Gonzalez-Garcia J., Lipovsky B., Floyd M. and Funning G.; 2014: *El Mayor-Cucapah (M_W 7.2) earthquake: early near-field postseismic deformation from InSAR and GPS observations*. J. Geophys. Res., Solid Earth, **119**, 1482-1497, doi:10.1002/2013JB010193.

Gourmelen N., Amelung F. and Lanari R.; 2010: *Interferometric synthetic aperture radar-GPS integration: interseismic strain accumulation across the Hunter Mountain Fault in the eastern California shear zone*. J. Geophys. Res., **115**, B09408, doi:10.1029/2009jb007064.

Gu G.H., Wang W.X., Xu Y.R. and Li W.J.; 2009: *Horizontal crustal movement before the Great Wenchuan earthquake obtained from GPS observations in the regional network*. Earthquake Sci., **22**, 471-478.

Hashimoto M.; 2013: *Crustal deformation associated with the 2011 Tohoku-oki earthquake: an overview.* Earthquake Spectra, **29**, S81-S98, doi:10.1193/1.4000117.

Hearn E.H., Bürgmann R. and Reilinger R.E.; 2002: *Dynamics of Izmit earthquake postseismic deformation and loading of the Du¨zce earthquake hypocenter*. Bull. Seismol. Soc. Am., **92**, 172-193.

Hooper A. and Zebker H.; 2007: *Phase unwrapping in three dimensions with application to InSAR time series*. Journal of the Optical Society of America, A **24**, 2737–2747.

Hooper A., Bekaert D., Spaans K and Arıkan M.; 2012: *Recent advances in SAR interferometry time series analysis for measuring crustal deformation*. Tectonophysics, **514-517**, 1–13.

Hsu Y.J., Simons M., Avouac J.P., Galetzka J., Sieh K., Chlieh M., Natawidjaja D., Prawirodirdjo L. and Bock Y.; 2006: *Frictional afterslip following the 2005 Nias-Simeulue earthquake, Sumatra*. Sci., **312**, 1921-1926.

Hunstad I., Pepe A., Atzori S., Tolomei C., Salvi S. and Lanari R.; 2009: *Surface deformation in the Abruzzi region, central Italy, from multitemporal DInSAR analysis*. Geophys. J. Int., **178**, 1193-1197.

Hyndman R.D. and Wang K.; 1993: *Thermal constraints on the zone of major thrust earthquake failure: the Cascadia subduction zone*. J. Geophys. Res., **98**, 2039-2060.

Jacobs A., Sandwell D., Fialko Y. and Sichoix L.; 2002: *The 1999 MW 7.1 Hector Mine, California earthquake: near-field postseismic deformation from ERS interferometry*. Bull. Seismol. Soc. Am., **92**, 1433-1442.

Jolivet R., Lasserre C., Doin M.P., Peltzer G., Avouac J.P., Sun J. and Dailu R.; 2013: *Spatio-temporal evolution of aseismic slip along the Haiyuan Fault, China: implications for fault frictional properties*. Earth Planet. Sci. Lett., **377**, 23-33.

Jonsson S., Segall P., Pederson R. and Bjornsson G.; 2003: *Post-earthquake ground movements correlated to pore-pressure transients*. Nature, **424**, 179-183.

Kaneko Y., Fialko Y., Sandwell D.T., Tong X. and Furuya M.; 2013: *Interseismic deformation and creep along the central section of the North Anatolian Fault (Turkey): InSAR observations and implications for rate-and-state friction properties*. J. Geophys. Res., Solid Earth, **118**, 316-331.

Lanari R., Mora O., Manunta M., Mallorqui J.J., Berardino P. and Sansosti E.; 2004: *A small-baseline approach for investigating deformations on full-resolution differential SAR interferograms*. IEEE Trans. Geosci. Remote Sens., **42**, 1377-1386.

Lanari R., Casu F., Manzo M., Zeni G., Berardino P., Manunta M. and Pepe A.; 2007: *An overview of the small baseline subset algorithm: a DInSAR technique for surface deformation analysis*. Pure Appl. Geophys., **164**, 637-661.

Larson K.M., Lowry A.R., Kostoglodov V., Hutton W., Sánchez O., Hudnut K. and Suárez G.; 2004: *Crustal deformation measurements in Guerrero, Mexico*. J. Geophys. Res., **109**, B04409.

Linde A.T. and Sacks I.S.; 2002: *Slow earthquakes and great earthquakes along the Nankai trough*. Earth Planet. Sci. Lett., **203**, 265-275.

Liu Y. and Rice J.R.; 2007: *Spontaneous and triggered aseismic deformation transients in a subduction fault model*. J. Geophys. Res., **112**, B09404.

Manzo M., Fialko Y., Casu F., Pepe A. and Lanari R.; 2012: *A quantitative assessment of DInSAR measurements of interseismic deformation: the southern San Andreas Fault case study*. Pure Appl. Geophys., **169**, 1463-1482.

Massonnet D., Rossi M., Carmona C., Adragna F., Peltzer G., Feigl K. and Rabaute T.; 1993: *The displacement field of the Landers earthquake mapped by radar interferometry*. Nature, **364**,138-142.

Massonnet D., Feigl K., Rossi M. and Adragna F.; 1994: *Radar interferometric mapping of deformation in the year after the Landers earthquake*. Nature, **369**, 227-230.

Miachkin V.I., Brace W.F., Sobolev G.A. and Dieterich J.H.; 1975: *Two models for earthquake forerunners*. Pure Appl. Geophys., **113**, 169-181.

Miyazaki S., McGuire J.J. and Segall P.; 2003: *A transient subduction zone slip episode in southwest Japan observed by the nationwide GPS array*. J. Geophys. Res., **108**, 2087, doi:10.1029/2001JB000456.

Miyazaki S., Segall P., Fukuda J. and Kato T.; 2004: *Space time distributions of afterslip following the 2003 Tokachi-Oki earthquake: implications for variations in fault zone frictional properties*. Geophys. Res. Lett., **31**, L06623, doi:10.1029/2003GL019410.

Miyazaki S., McGuire J.J. and Segall P.; 2011: *Seismic and aseismic fault slip before and during the 2011 off the Pacific coast of Tohoku earthquake*. Earth Planets Space, **63**, 637-642, doi:10.504/eps.2011.07.001.

Mogi K.; 1985a: *Earthquake prediction*. Academic Press, Tokyo, Japan, 355 pp.

Mogi K.; 1985b: *Temporal variation of crustal deformation during the days preceding a thrust-type great earthquake — The 1944 Tonankai earthquake of magnitude 8.1, Japan*. Earthquake Prediction, Pure Appl. Geophys., **122**, 765-780.

Motagh M., Hoffmann J., Kampes B., Baes M. and Zschau J.; 2007: *Strain accumulation across the Gazikoy–Saros segment of the North Anatolian Fault inferred from Persistent Scatterer Interferometry and GPS measurements*. Earth Planet. Sci. Lett., **255**, 432-444, doi:10.1016/j.epsl.2007.01.003.

Nur A.; 1972: *Dilatancy, pore fluids, and premonitory variation of ts/tp travel times*. Bull. Seismol. Soc. Am., **62**, 1217-1222.

Ozawa S., Murakami M., Kaidzu M., Tada T., Sagiya T., Hatanaka Y., Yarai H. and Nishimura T.; 2002: *Detection and monitoring of on going aseismic slip in the Tokai region, central Japan*. Sci., **298**, 1009-1012.

Ozawa S., Nishimura T., Munekane H., Suito H., Kobayashi T., Tobita M. and Imakiire T.; 2012: *Preceding, coseismic, and postseismic slips of the 2011 Tohoku earthquake, Japan*. J. Geophys. Res., **117**, B07404, doi:10.1029/2011JB009120.

Peltzer G., Crampé F., Hensley S. and Rosen P.; 2001: *Transient strain accumulation and fault interaction in the eastern California shear zone*. Geol. Soc. Am., **29**, 975-978.

Peng Z. and Gomberg J.; 2010: *An integrated perspective of the continuum between earthquakes and slow-slip phenomena*. Nature Geosci., **3**, 599-607.

Peyret M., Dominguez S., Cattin R., Champenois J., Leroy M. and Zajac A.; 2011: *Present-day interseismic surface deformation along the Longitudinal Valley, eastern Taiwan, from a PS-InSAR analysis of the ERS satellite archive*. J. Geophys. Res., **116**, B03402.

Pezzo G., Tolomei C., Atzori S., Salvi S., Shabanian E., Bellier O. and Farbod Y.; 2012: *New kinematic constraints of the western Doruneh Fault, northeastern Iran, from interseismic deformation analysis*. Geophys. J. Int., **190**, 622-628. doi:10.1111/j.1365-246X.2012.05509.

Pezzo G., Merryman Boncori J.P., Tolomei C., Salvi S., Atzori S., Antonioli A., Trasatti E., Novali F., Serpelloni E., Candela L. and Giuliani R.; 2013: *Coseismic deformation and source modeling of the May 2012 Emilia (northern Italy) earthquakes*. Seismol. Res. Lett., **84**, 645-655, doi:10.1785/0220120171.

Pollitz F.; 2005: *Transient rheology of the upper mantle beneath central Alaska inferred from the crustal velocity field following the 2002 Denali earthquake*. J. Geophys. Res., **110**, B08407.

Pollitz F.F., Peltzer G. and Bürgmann R.; 2000: *Mobility of continental mantle: evidence from postseismic geodetic observations following the 1992 Landers earthquake*. J. Geophys. Res., Solid Earth, **105**, 8035-8054.

Pollitz F., Wicks C. and Thatcher R.; 2001: *Mantle flow beneath a continental strikeslip fault: postseismic deformation after the 1999 Hector Mine earthquake*. Sci., **293**, 1814-1818.

Pritchard M.E. and Simons M.; 2006: *An aseismic slip pulse in northern Chile and along-strike variations in seismogenic behavior*. J. Geophys. Res., **111**, B08405, doi:10.1029/2006JB004258.

Reale D., Nitti D.O., Peduto D., Nutricato R., Bovenga F. and Fornaro G.; 2011: *Postseismic deformation monitoring with the COSMO/SKYMED constellation*. IEEE Geosci. Remote Sens. Lett., **8**, 696-700.

Reid H.F.; 1910: *The mechanics of the earthquake*, vol. II. In: Lawson A.C. (chairman), The California earthquake of April 18, 1906, Report of the State Earthquake Investigation Commission, Carnegie Institution of Washington, Washington, DC, USA, Publ. 87, 192 pp. (reprinted in 1969).

Roeloffs E.A.; 2006: *Evidence for aseismic deformation rate changes prior to earthquakes*. Ann. Rev. Earth Planet. Sci., **34**, 591-627.

Ryder I., Parsons B., Wright T.J. and Funning G.J.; 2007: *Postseismic motion following the 1997 Manyi (Tibet) earthquake: InSAR observations and modelling*. Geophys. J. Int., **169**, 1009-1027.

Salvi S., Atzori S., Merryman Boncori J.P., Tolomei C. and Zoffoli S.; 2011: *Observing the great Tohoku earthquake by the COSMO-SkyMed operational satellites*. Space Res. Today, **181**, 25-27, doi:10.1016/j.srt.2011.07.008.

Salvi S., Atzori S., Tolomei C., Antonioli A., Trasatti E., Merryman Boncori J.P., Pezzo G., Coletta A. and Zoffoli S.; 2012a: *Results from INSAR monitoring of the 2010-2011 New Zealand seismic sequence: EA detection and earthquake triggering*. In: Proc. IEEE Int. Geosci. Remote Sens. Symp., Munich, Germany, pp. 3544-3547.

Salvi S., Stramondo S., Funning G.J., Ferretti A., Sarti F. and Mouratidis A.; 2012b: *The Sentinel-1 mission for the improvement of the scientific understanding and the operational monitoring of the seismic cycle*. Remote Sens. Environ., **120**, 164-174.

Scholz C.H., Sykes L.R. and Aggarwal Y.P.; 1973: *Earthquake prediction: a physical basis*. Sci., **181**, 803-810.

Steacy S., Gomberg J. and Cocco M.; 2005: *Introduction to special section: stress dependent seismic hazard*. J. Geophys. Res., **110**, B05S01, doi:10.1029/2005JB003692.

Szeliga W., Bilham R., Kakar D.M. and Lodi S.H.; 2012: *Interseismic strain accumulation along the western boundary of the Indian subcontinent*. J. Geophys. Res., **117**, B08404, doi:10.1029/2011JB008822.

Thatcher W.; 1983: *Nonlinear strain buildup and the earthquake cycle on the San Andreas Fault*. J. Geophys. Res., **8**, 5893-5902, doi:10.1029/JB088iB07p05893.

Torres R., Snoeij P., Geudtner D., Bibby D., Davidson M., Attema E. and Rostan F.; 2012: *GMES Sentinel-1 mission*. Remote Sens. Environ., **120**, 9-24.

Walters R.J., Holley R.J., Parsons B. and Wright T.J; 2011: *Interseismic strain accumulation across the North Anatolian Fault from Envisat InSAR measurements*. Geophys. Res. Lett., **38**, L05303, doi:10.1029/2010GL046443.

Wang K.; 2007: *Elastic and viscoelastic models of crustal deformation in subduction earthquake cycles*. In: Dixon T. and Moore J. (eds), The seismogenic zone of subduction thrust faults, Columbia University Press, New York, NY, USA, pp. 540-575.

Wang H. and Wright T.J.; 2012: *Satellite geodetic imaging reveals internal deformation of western Tibet*. Geophys. Res. Lett., **39**, L07303, doi:10.1029/2012GL051222.

Wang H., Wright T.J. and Biggs J.; 2009: *Interseismic slip rate of the northwestern Xianshuihe fault from InSAR data*. Geophys. Res. Lett., **36**, L03302, doi: 10.1029/2008GL036560.

Weston J., Ferreira A.M.G. and Funning G.J.; 2011: *Global compilation of interferometric synthetic aperture radar earthquake source models: 1. Comparisons with seismic catalogs*. J. Geophys. Res., **116**, B08408, doi:10.1029/2010JB008131.

Wright T.J., Parsons B. and Fielding E.; 2001: *Mesurement of interseismic strain accumulation across the North Anatolian Fault by satellite radar interferometry*. Geophys. Res. Lett., **28**, 2117-2120.

Yu S.B., Kuo L.C., Hsu Y.J., Su H.H., Liu C.C., Hou C.S., Lee J.F., Lai T.C., Liu C.C., Liu C.L., Tseng T.F., Tsai C.S. and Shin T.C.; 2001: *Preseismic deformation and coseismic displacements associated with the 1999 Chi-Chi, Taiwan, earthquake*. Bull. Seismol. Soc. Am., **91**, 995-1012.

Zebker H.A. and Villasenor J.; 1992: *Decorrelation in interferometric radar echoes*. IEEE Trans. Geosci. Remote Sens., **30**, 950-959.

Zebker H.A., Rosen P.A., Goldstein R.M., Gabriel A. and Werner C.L.; 1994: *On the derivation of coseismic displacement fields using differential radar interferometry: the Landers earthquake*. J. Geophys. Res., **99**, 19617-19634.

Corresponding author: Cristiano Tolomei
Istituto Nazionale di Geofisica e Vulcanologia
Via di Vigna Murata 605, 00143 Roma, Italy
Phone: +39 06 51860384; fax: +39 06 51860541; e-mail: cristiano.tolomei@ingv.it